Research Square

Preprints are preliminary reports that have not undergone peer review.
They should not be considered conclusive, used to inform clinical practice,
or referenced by the media as validated information.

# Organocatalytic enantioselective cycloaddition of naphthoquinone methides

**Xin-Qi Zhu**

xinqizhu@ynnu.edu.cn

Yunnan Normal University https://orcid.org/0009-0006-7488-8251

**Zhao-Tai Chen**

Yunnan Normal University

**Hai-Yu Yang**

Yunnan Normal University

**Kai-Yu Fan**

Yunnan Normal University

**Longwu Ye**

Xiamen University https://orcid.org/0000-0003-3108-2611

**Article**

**Keywords:**

**Posted Date:** February 26th, 2026

**DOI:** https://doi.org/10.21203/rs.3.rs-8915583/v1

**License:** This work is licensed under a Creative Commons Attribution 4.0 International License.
Read Full License

**Additional Declarations:** There is **NO** Competing Interest.

# Abstract

Quinone methides and their *aza*-analogues represent the pivotal intermediates in asymmetric synthesis. However, catalytic enantioselective reactions of extended naphthalene-based analogues including naphthoquinone methides (Nap-QMs) and *aza*-naphthoquinone methides (*aza*-Nap-QMs) remain underdeveloped and are limited to nucleophilic additions. Herein, we report an organocatalytic asymmetric [4 + 2] cycloaddition of enamides with Nap-QMs and *aza*-Nap-QMs, providing an efficient access to a diverse range of tricyclic phenalene derivatives bearing chiral tertiary amines with excellent remote stereocontrol. Furthermore, a CPA/Ag-catalyzed tandem cycloaddition/cyclization enables an asymmetric relay reaction, affording chiral dihydrobenzo[*e*]indoles and 1,2-dihydronaphtho[2,1-*b*]furans with high enantioselectivities. This protocol not only represents the first asymmetric cycloaddition and relay cyclization of (*aza*)-Nap-QMs, but also constitutes the first asymmetric synthesis of chiral dihydrophenalenes.


# Introduction

Quinone methides (QMs)[1–3] and *aza*-quinone methides (*aza*-QMs)[4–6] have emerged as versatile and valuable synthetic intermediates for the construction of versatile chiral molecules in catalytic asymmetric synthesis[7–11]. In the past decades, the use of chiral Brønsted acids[12–20] has enabled a range of stereoselective asymmetric reactions involving QMs and *aza*-QMs generated in situ from the corresponding hydroxybenzyl alcohols and aminobenzyl alcohols. This approach includes asymmetric nucleophilic additions[21–31] and asymmetric cycloadditions[32–42], offering efficient routes for the synthesis of functionalized chiral phenols, anilines and heterocycles (Fig. 1a). Nevertheless, catalytic enantioselective reactions involving extended analogues of QMs, where the carbonyl and methide units are embedded in separate aromatic rings, remain scarce (Fig. 1b). In 2023, Sun and colleagues first reported an elegant chiral phosphoric acids (CPA) catalyzed remote asymmetric nucleophilic addition using naphthoquinone methides (Nap-QMs) and *aza*-naphthoquinone methides (*aza*-Nap-QMs), generated in situ from 8-(hydroxyarylmethyl)naphthalen-2-ols and 2-naphthylamine derivatives[43]. Almost at the same time, Li et al. developed a CPA-catalyzed asymmetric nucleophilic addition of 2-naphthoquinone-6-methides, formed in situ from 6-(hydroxydiarylmethyl)naphthalen-2-ols, leading to the synthesis of chiral tetraarylmethanes with excellent enantioselectivities[44]. Very recently, similar strategies for asymmetric nucleophilic additions involving Nap-QMs were also exploited by Sun[45] and Li[46,47], respectively. Notably, these advances highlight the utility of naphthoquinone methides (Nap-QMs) as a promising platform for assembling enantioenriched, structurally complex target molecules. Despite these significant advances (Fig. 1b), these protocols are limited to the asymmetric nucleophilic addition of Nap-QMs, while their catalytic asymmetric cycloaddition for assembling naphthalene-based chiral polycyclic frameworks remains unexploited (Fig. 1c), with only one example on racemic cycloaddition of Nap-QMs via achiral scandium catalysis by Liu[48].

As versatile synthetic building blocks in organic synthesis, enamides have garnered significant attention over the past decades for the construction of diverse biological and pharmaceutical molecules[49–53]. In particular, enamides serve as difunctionalized synthons in catalytic asymmetric reactions, and their asymmetric cycloadditions are particularly valuable for preparing useful chiral cyclic compounds and chiral amines. By utilizing this strategy, various asymmetric cycloadditions of enamides with (*aza*)-QMs have been established for the synthesis of valuable chiral heterocycles[54–56]. Inspired by these results, we hypothesized that enamides might

serve as difunctionalized synthons to engage in a remote asymmetric cycloaddition with (*aza*)-Nap-QMs, leading to the formation of naphthalene-based chiral polycyclic products (Fig. 1c). However, significant challenges can be anticipated in achieving this asymmetric cycloaddition of (*aza*)-Nap-QMs: (i) how to prevent competing background nucleophilic addition of (*aza*)-Nap-QMs; (ii) how to control enantioselectivity, particularly remote stereocontrol, during the formation of a new ring; and (iii) how to suppress the competing hydrolysis of enamides, which leads to the formation of ketone byproducts. Herein, we report an organocatalytic enantioselective [4 + 2] cycloaddition of (*aza*)-Nap-QMs with enamides, which provides efficient access to a wide range of tricyclic phenalene derivatives bearing chiral tertiary amines[57,58] with excellent remote stereocontrol. Interestingly, the asymmetric relay reaction[59–61], proceeding through a CPA/Ag-catalyzed tandem cycloaddition/cyclization of (*aza*)-Nap-QMs with enamides, allows the highly enantioselective formation of chiral dihydronaphtho[2,1-*b*]furans and 1,2-dihydrobenzo[*e*]indoles. Importantly, this protocol not only represents the first catalytic asymmetric cycloaddition of (*aza*)-Nap-QMs, but also constitutes the first asymmetric relay cyclization of (*aza*)-Nap-QMs and the first asymmetric synthesis of chiral dihydrophenalenes. It is noteworthy that phenalene derivatives, dihydronaphtho[2,1-*b*]furans and 1,2-dihydrobenzo[*e*]indoles are privileged structural motifs prevalent in numerous natural products and bioactive molecules (Fig. 2)[62–67].

# Results and discussion

We commenced our investigation by employing 8-(hydroxy(4-methoxyphenyl)methyl)naphthalen-2-ol **1a** and alkyne-tethered TFA-protected[68,69] enamide **2a** as model substrates to explore the asymmetric cycloaddition of Nap-QMs. Selected optimization results are summarized in Table 1. In the presence of 10 mol % CPA **A1** as the catalyst and DCE as the solvent at room temperature, we were pleased to find that the expected chiral cycloadduct **3a** was obtained in excellent yield with 90% ee (Table 1, entry 1). Subsequent screening of various CPA catalysts **A2–A8** maintained excellent yields but did not improve enantioselectivity (Table 1, entries 2–8). Then, the use of spiro-CPA **A9** and *N*-triflyl phosphoramide **A10** led to excellent yield, but only low enantioselectivity was obtained (Table 1, entries 9 and 10). Further evaluation of some other typical solvents such as DCM, chloroform, toluene and PhF (Table 1, entries 11–14), and found that the use of PhF as solvent could further slightly improve the enantioselectivity (Table 1, entry 13). To our delight, an obvious temperature effect was observed, and the chiral dihydrophenalene **3a** was formed in 92% yield with 93% ee when the temperature was lowered to 0°C

(Table 1, entry 15). Of note, only one diastereoisomer (dr > 20:1) was observed in this asymmetric cycloaddition.

After establishing the optimal reaction conditions (Table 1, entry 15), we proceeded to investigate the substrate scope of this catalytic asymmetric cycloaddition involving Nap-QMs. As shown in Fig. 3, we initially examined various 4-arylethynyl-substituted enamides under the optimized conditions. It was found that electron-donating groups at the *para*-position of the phenyl ring of the enamides had little influence on this annulation, furnishing the corresponding chiral dihydrophenalenes **3a–3f** in 82–93% yields with excellent enantioselectivities (90–94% ees). We also evaluated enamides bearing electron-withdrawing substituents such as F and Cl, which efficiently yielded the corresponding chiral dihydrophenalenes **3g** (92% yield, 96% ee) and **3h** (94% yield, 91% ee), respectively. Additionally, aryl groups with functional groups, such as $CF_3$ and ester group, were well tolerated in the cycloaddition, providing the desired chiral products **3i** and **3j** in excellent yields with high enantioselectivities. Next, enamides with *meta*- and *ortho*-substituents on the aromatic ring were also found to be suitable substrates, yielding the corresponding products **3k–3n** with good to excellent yields and high enantioselectivities. We then examined enamides containing disubstituted aromatic groups (**2o–2r**), which efficiently afforded the corresponding chiral dihydrophenalenes **3o–3r** in 82–95% yields with 78–94% ees. Furthermore, the asymmetric cycloaddition proceeded smoothly with naphthalene- and heterocycle-linked enamides (**2s–2u**), delivering the desired cycloaddition products **3s–3u** in near-quantitative yields and 92–98% ees. Alkyl-substituted enamides **2v** and **2w** were also proven to be applicable substrates, providing the expected chiral dihydrophenalenes **3v** and **3w** in high yields with excellent enantioselectivities. Notably, the reaction was also extended to enamides without phenylethynyl substitutions, such as those with phenyl and styryl groups, which furnished the corresponding chiral dihydrophenalenes **3x–3ab** in moderate to good yields with high enantioselectivities. We next screened a range of 2-naphthol derivatives **1** bearing a benzylic alcohol unit, which efficiently participated in this enantioselective cycloaddition, affording the corresponding chiral dihydrophenalenes **3ac–3ag** in 91–98% yields with 70–94% ees. Importantly, *aza*-Nap-QMs generated in situ from 2-naphthylamine derivatives were also found to be competent substrates for this transformation, leading to the 2-naphthylamine-derived chiral dihydrophenalenes **3ah** and **3ai** in good yields with high enantioselectivities. Interestingly, this asymmetric annulation could be successfully extended to enamides bearing complex pharmaceutical scaffolds. For instance, adapalene-, indomethacin-, and isoxepac-derived enamides served as suitable substrates, furnishing the corresponding drug-derived dihydrophenalenes **3aj–3al** in excellent yields (87–98%) and enantioselectivities (92–94% ees). Moreover, the dehydrocholic acid-derived enamide could be smoothly converted into the more complex chiral polycyclic product **3am** in good yield. Of note, excellent diastereoselectivities (dr > 20:1) were all obtained in all cases. However, when enamide bearing a trisubstituted olefin moiety was employed, the reaction gave a complex mixture, and no desired dihydrophenalene was

detected (see Supplementary Fig. 1). Thus, this protocol constitutes the first catalytic asymmetric cycloaddition of Nap-QMs and *aza*-Nap-QMs.

In consideration of the chiral dihydrophenalenes **3** contain both alkyne and naphthol functional groups, we envisioned that these products could undergo a one-pot asymmetric relay cyclization by transition-metal catalysis to form chiral tetracyclic compounds. To explore this possibility, we selected 8-(hydroxy(4-methoxyphenyl)methyl)naphthalen-2-ol **1a** and the alkyne-tethered enamide **2a** as model substrates. A selection of the results is presented in Table 2. Initially, the reaction was conducted under the standard conditions (Table 1, Entry 14), and various transition-metal catalysts, including $Cu(MeCN)_4PF_6$, $Pd(OAc)_2$, $PdCl_2$, $IPrAuNTf_2$, and $Ag_2O$, were screened (Table 2, entries 1–5). We were delighted to find that the use of silver catalyst $Ag_2O$ could undergo 5-*endo-dig* cyclization[70] to deliver the desired 1,2-dihydronaphtho[2,1-*b*]furan **4a** in 80% yield with excellent enantioselectivity (Table 2, entry 5). Other silver salts, such as $AgNTf_2$ and AgOTf, proved less effective (Table 2, entries 6 and 7). Notably, the addition of $K_2CO_3$ (2 equiv) significantly improved the yield, delivering product **4a** in 92% yield with 94% ee (Table 2, entry 10). It is worthy noting that under these one-pot asymmetric relay cyclization conditions involving Nap-QMs, only the 5-*endo*-dig cyclization product was observed, the corresponding 6-*exo*-dig cyclization product was not detected.

With the optimal reaction conditions established (Table 2, entry 10), the substrate scope of this one-pot asymmetric relay cyclization of Nap-QMs was investigated. As illustrated in Fig. 4, we first explored various alkyne-tethered enamides bearing either electron-donating or electron-withdrawing substituents at the *para*-position of the phenyl ring, and found that the desired chiral 1,2-dihydronaphtho[2,1-*b*]furans **4a**–**4h** were furnished in 48–94% yields with 90–96% ees. Furthermore, this asymmetric relay cyclization could also proceed smoothly with the functional groups such as $CF_3$ and $CO_2Me$, providing the corresponding products **4i** (79% yield, 97% ee) and **4j** (86% yield, 96% ee), respectively. Enamides bearing *meta*- or *ortho*-substitutions also proved to be appropriate substrates, yielding the corresponding enantioenriched 1,2-dihydronaphtho[2,1-*b*]furans **4k**–**4m** in moderate to good yields with the ees of 90–94%. Additionally, disubstituted and naphthyl-substituted enamides reacted efficiently with Nap-QMs to deliver the anticipated tetracyclic products **4n–4q** in 66–96% yields with 84–95% ees. Next, the reaction was extended to heterocycle-substituted enamides, such as those bearing thiophene and benzofuran groups, providing the corresponding enantioenriched products **4r** and **4s** in moderate yields with excellent enantioselectivities. Subsequently, we examined various Nap-QM precursors in this asymmetric relay cyclization. Naphthols **1** bearing either thiomethyl and fluoro substituents on the phenyl ring or a methoxy substituent on the naphthyl ring were also found to be suitable, yielding the desired chiral 1,2-dihydronaphtho[2,1-*b*]furans **4t–4v** in high yields with good enantioselectivities. Again, excellent diastereoselectivities (dr > 20:1) were achieved in all cases. It is notable that the 6-*exo*-dig cyclization product was not observed in all products. The absolute configuration of product **4v** was confirmed by X-ray crystallographic analysis, and those of the other products were assigned by analogy, thereby confirming the absolute configurations of products **3** in Fig. 3.

Interestingly, this one-pot asymmetric relay cyclization could also be extended to *aza*-Nap-QMs, efficiently delivering the valuable chiral dihydrobenzo[*e*]indoles **5** under the standard conditions (Table 2, entry 10). The substrate scope is depicted in Fig. 5. We first evaluated various protected naphthylamine

derivatives **1** in the asymmetric relay cyclization with enamide **2a**. The phenylacetyl (BnCO–) protecting group gave the optimal

result (77% yield, dr > 20:1, 92% ee). Subsequently, a range of enamides bearing electron-donating or electron-withdrawing substituents at different positions on the phenyl ring were examined, affording the corresponding chiral tetracyclic dihydrobenzo[*e*]indoles **5a–5g** in moderate to excellent yields with excellent diastereo- and enantioselectivities. Naphthylamines bearing a fluoro substituent on the phenyl ring were also tolerated, yielding the expected product **5h** in 79% yield with 70% ee. This work therefore represents the first asymmetric relay cyclization involving Nap-QMs and *aza*-Nap-QMs.

To demonstrate the synthetic utility of this methodology, the preparative-scale reactions and further product transformations were investigated (Fig. 6). Preparative-scale synthesis of chiral dihydrophenalene **3a** and 1,2-dihydronaphtho[2,1-*b*]furan **4a** was first carried out, and the desired products **3a** (0.79 g, 99%, 94% ee) and **4a** (0.71 g, 89%, 94% ee) were synthesized respectively under standard reaction condition, as shown in Fig. 6a. Subsequently, derivatization of the hydroxyl group in the naphthol moiety of **3a** with $Tf_2O$ provided the Tf-protected product **6a** in 68% yield with 92% ee, which could undergo the further facile cross coupling reaction. Treatment of **3a** with $Cs_2CO_3$ induced elimination of the trifluoroacetamide group, yielding phenalenone product **6b** in 74% yield. It's worth noting that the dearomatization of naphthol moiety and rearomatization occurred in this elimination procedure. Further transformations of 1,2-dihydronaphtho[2,1-*b*]furan **4a** were also explored. $RuCl_3$-catalyzed oxidation of the olefin moiety using $NaIO_4$ afforded ketone **6c** in moderate yield with good diastereoselectivity and enantioselectivity. Interestingly, reduction of **4a** with $Et_3SiH$ promoted by $BF_3{\cdot}Et_2O$ proceeded via a reduction/elimination cascade to furnish chiral naphtho[2,1-*b*]furan **6d** in 99% yield with 95% ee. Importantly, almost no erosion of the enantiopurity of the compounds was observed in all these elaborations.

# Mechanistic investigations

To further elucidate the reaction mechanism, a series of control experiments were conducted (Fig. 7). First, treatment of dihydrophenalene **3a** with $Ag_2O$ catalyst alone catalyzed the 5-*endo*-dig cyclization to afford 1,2-dihydronaphtho[2,1-*b*]furan **4a** in 100 min (Fig. 7a). When both $Ag_2O$ and chiral phosphoric acid (CPA) **A1**

were used as cocatalysts, the cyclization time was reduced to 32 min (Fig. 7b). In contrast, employing the preformed CPA-Ag complex as the catalyst afforded **4a** in 71% yield with 94% ee, but required a much longer reaction time (17 h, Fig. 7c). These results suggest that CPA assists the second 5-*endo*-dig cyclization to form **4a**, and that the CPA-Ag complex is not the key catalytic species in this step. Moreover, when the free hydroxyl group of the naphthol was blocked with methyl (**1a'**), only dimerization product was obtained and no cycloaddition product was detected, underscoring the essential role of the free hydroxyl group in naphthols **1** (Fig. 7d). Reaction of **1a** with deuterium-labeled enamide **[D]-2b** under standard conditions furnished **[D]-3b** with complete deuterium retention at the methylene position

(Fig. 7e). Finally, a linear correlation was observed between the ee of product **3a** and the ee of catalyst **A1**, indicating that the enantioselectivity-determining step involves only a single CPA molecule (Fig. 7f). This linear relationship contrasts with that reported by Sun et al. in 2023[43].

On the basis of the foregoing mechanistic experiments and prior reports on CPA-catalyzed reactions of Nap-QMs[43–47], a plausible mechanism for the present asymmetric cycloaddition and relay cyclization is proposed (Fig. 8). Initially, CPA catalyst **A1** engages 8-(hydroxy(4-methoxyphenyl)methyl)naphthalen-2-ol **1a** through dual hydrogen-bonding interactions to form intermediate **A**, which undergoes dehydration assisted by CPA catalyst, affording the key Nap-QM intermediate **B**. Then CPA catalyst directs the enantioselective remote 1,6-addition of enamide **2a** to intermediate **B** via double hydrogen-bonding interactions, yielding intermediate **C**, which is the enantioselectivity-determining step. Intermediate **C** then undergoes an intramolecular Mannich reaction accompanied by dearomatization of the naphthol ring, leading to cyclized intermediate **D**. Subsequently, the aromatization of intermediate **D** assisted by CPA catalyst **A1** generates cycloaddition product **3a** and regenerate the catalyst **A1**, thereby completing the first catalytic cycle. The second catalytic cycle proceeds in the presence of $Ag_2O$ and CPA **A1**. Activation of the phenylethynyl group of **3a** by silver furnishes intermediate **E**, while the naphthol hydroxyl group is simultaneously activated by CPA via hydrogen-bonding. Intermediate **E** then undergoes an intramolecular 5-*endo*-dig cyclization to give tetracyclic intermediate **F**, which goes through proton demetalation to deliver the final 1,2-dihydronaphtho[2,1-*b*]furan **4a**. This protocol represents a rare example of a CPA catalyst playing a triple role through hydrogen bonding interactions.

# Conclusions

In summary, we have developed the organocatalytic asymmetric [4 + 2] cycloaddition of naphthoquinone methides (Nap-QMs) and their *aza*-analogues (*aza*-Nap-QMs) with enamides, efficiently constructing a diverse range of tricyclic dihydrophenalene derivatives featuring chiral tertiary amine centers with excellent remote stereocontrol. Furthermore, a tandem cycloaddition/cyclization strategy enabled by CPA/silver cooperative catalysis realizes an asymmetric relay reaction, affording 1,2-dihydronaphtho[2,1-*b*]furans and chiral dihydrobenzo[*e*]indoles with high enantioselectivity. This work not only breaks the previous limitation of asymmetric transformations involving (*aza*)-Nap-QMs to nucleophilic additions, representing their first asymmetric cycloaddition and relay cyclization reactions, but also constitutes the first asymmetric synthesis of chiral dihydrophenalene derivatives. We believe that these findings will offer new perspectives and further explorations in the field of asymmetric catalysis based on cycloaddition reaction via the remote control and Nap-QM chemistry.

# Methods

**General**. For $^{1}H$ and $^{13}C$ nuclear magnetic resonance (NMR) spectra of compounds in this manuscript and details of the synthetic procedures as well as more reaction condition screening, see Supplementary Information.

**General procedure for the synthesis of chiral dihydrophenalenes 3.** A 10 mL reaction tube was charged with chiral phosphoric acid **A1** (10 mol %, 0.02 mmol, 15 mg), **1** (0.2 mmol) and **2** (1.2 equiv, 0.24 mmol), PhF (2 mL) were added sequentially. The reaction mixture was then stirred at 0°C. After completion of the reaction (monitored by TLC), the reaction mixture was concentrated under vacuum and purified by column chromatography on silica gel, eluting with EtOAc/hexane to afford the products **3**.

**General procedure for the synthesis of chiral 1,2-dihydronaphtho[2,1- b ]furans 4.** A 10 mL reaction tube was charged with chiral phosphoric acid **A1** (10 mol %, 0.02 mmol, 15 mg), **1** (1.2 equiv, 0.24 mmol) and **2** (0.2 mmol), PhF (6 mL) were added sequentially. The reaction mixture was then stirred at 0°C. After completion of the reaction (monitored by TLC), $Ag_2O$ (20 mol %, 0.04 mmol, 9.3 mg) and $K_2CO_3$ (2 equiv, 0.4 mmol, 55.3 mg) were added sequentially, the reaction mixture was then stirred at room temperature. After completion of the reaction (monitored by TLC), the reaction mixture was concentrated under vacuum and purified by column chromatography on silica gel, eluting with EtOAc/hexane to afford the products **4**.

**General procedure for the synthesis of chiral dihydrobenzo[ e ]indoles 5.** A 10 mL reaction tube was charged with chiral phosphoric acid **A1** (10 mol %, 0.02 mmol, 15 mg), **1** (1.2 equiv, 0.24 mmol) and **2** (0.2 mmol), PhF (6 mL) were added sequentially. The reaction mixture was then stirred at 0°C. After completion of the reaction (monitored by TLC), $Ag_2O$ (20 mol %, 0.04 mmol, 9.3 mg) and $K_2CO_3$ (2 equiv, 0.4 mmol, 55.3 mg) were added sequentially, the reaction mixture was then stirred at room temperature. After completion of the reaction (monitored by TLC), the reaction mixture was concentrated under vacuum and purified by column chromatography on silica gel, eluting with EtOAc/hexane to afford the products **5**.

## Declarations

# Reprints and permissions information

is available online at www.nature.com/reprints.

### Correspondence and requests

for materials should be addressed to X.-Q.Z.

# Competing interests:

The authors declare no competing interests.

# Author contributions

Z.-T.C., H.-Y.Y. and K.-Y. F. performed experiments. L.-W.Y. and X.-Q.Z. conceived and directed the project and wrote the paper. All authors discussed the results and commented on the manuscript.

# Acknowledgements

We are grateful for financial support from the National Natural Science Foundation of China (22125108, 22331004 and 22121001 for L.-W.Y.), Expert Workstation in Yunnan Province (202405AF140035, L.-W.Y.), the Yunnan Key Laboratory of Modern Separation Analysis and Substance Transformation (202449CE340001, X.-Q.Z.), the Yunnan Fundamental Research Project (202401CF070024, X.-Q.Z.). We also thank Professor Dr. Jieping Zhu (École Polytechnique Fédérale de Lausanne) for his support.

# Data availability.

Data for the crystal structures reported in this paper have been deposited at the Cambridge Crystallographic Data Centre (CCDC) under the deposition numbers 2528722 (**4v**). Copies of these data can be obtained free of charge via www.ccdc.cam.ac.uk/data_request/cif. All other data supporting the findings of this study, including experimental procedures and compound characterization, are available within the paper and its Supplementary Information files or from the corresponding authors on request.

## References

1. Gnaim S, Shabat D (2014) Quinone-methide species, a gateway to functional molecular systems: from self-immolative dendrimers to long-wavelength fluorescent dyes. Acc Chem Res 47:2970–2984
2. Willis NJ, Bray C (2012) D. *ortho*-Quinone methides in natural product synthesis. Chem Eur J 18:9160–9173
3. Van De Water RW, Pettus TR (2002) R. *o*-Quinone methides: intermediates underdeveloped and underutilized in organic synthesis. Tetrahedron 58:5367–5405
4. Li Y-L, Li Z-M, Wang K-K, He X-L (2024) Beyond 1,4-addition of in-situ generated (*aza*-)quinone methides and indole imine methides. Chin Chem Lett 35:109322
5. Liao H-H, Miñoza S, Lee S-C, Rueping M (2022) *Aza-ortho*-quinone methides as reactive intermediates: generation and utility in contemporary asymmetric synthesis. Chem Eur J 28:e202201112
6. Yang B, Gao S (2018) Recent advances in the application of Diels–Alder reactions involving *o*-quinodimethanes, *aza-o*-quinone methides and *o*-quinone methides in natural product total synthesis. *Chem. Soc. Rev.* 47, 7926–7953
7. Li X, Li Z, Sun J (2022) Quinone methides and indole imine methides as intermediates in enantioselective catalysis. Nat Synth 1:426–438

8. Qin W, Liu Y, Yan H (2022) Enantioselective synthesis of atropisomers via vinylidene *ortho*-quinone methides (VQMs). Acc Chem Res 55:2780–2795
9. Li W, Xu X, Zhang P, Li P (2018) Recent advances in the catalytic enantioselective reactions of *para*-Quinone methides. Chem Asian J 13:2350–2359
10. Dorsch C, Schneider C (2022) Asymmetric Brønsted acid catalyzed cycloadditions of *ortho*-quinone methides and related compounds. Synthesis 54:3125–3141
11. Wang Z, Sun J (2015) Recent advances in catalytic asymmetric reactions of *o*-quinone methides. Synthesis 47:3629–3644
12. Akiyama T (2007) Stronger Brønsted acids. Chem Rev 107:5744–5758
13. Parmar D, Sugiono E, Raja S, Rueping M (2014) Complete field guide to asymmetric BINOL-phosphate derived Brønsted acid and metal catalysis: history and classification by mode of activation; Brønsted acidity, hydrogen bonding, ion pairing, and metal phosphates. Chem Rev 114:9047–9153
14. Akiyama T, Mori K (2015) Stronger Brønsted acids: recent progress. Chem Rev 115:9277–9306
15. James T, Gemmeren M, List B (2015) Development and applications of disulfonimides in enantioselective organocatalysis. Chem Rev 115:9388–9409
16. Wang Y-B, Tan B (2018) Construction of axially chiral compounds via asymmetric organocatalysis. Acc Chem Res 51:534–547
17. Maji R, Mallojjala SC, Wheeler SE (2018) Chiral phosphoric acid catalysis: from numbers to insights. Chem Soc Rev 47:1142–1158
18. Zhang H-H, Shi F (2022) Organocatalytic atroposelective synthesis of indole derivatives bearing axial chirality: strategies and applications. Acc Chem Res 55:2562–2580
19. Schreyer L, Properzi R, List B (2019) IDPi catalysis. Angew Chem Int Ed 58:12761–12777
20. Betinol IO, Kuang Y, Mulley BP, Reid JP (2025) Controlling stereoselectivity with noncovalent interactions in chiral phosphoric acid organocatalysis. Chem Rev 125:4184–4286
21. Cui Y, Wang Y-B, Liu H-H, Xiang S-H, Tan B (2025) Organocatalytic activation of alkynes enabled remote control of atroposelectivity via vinylidene *para*-quinone methides. J Am Chem Soc 147:3450–3458
22. Xu H-L et al (2025) Organocatalytic asymmetric synthesis of *o*-carboranyl amines. J Am Chem Soc 147:3692–3701
23. Lin X et al (2024) Diastereo-divergent synthesis of chiral hindered ethers via a synergistic calcium(II)/gold(I) catalyzed cascade hydration/1,4-addition reaction. Nat Commun 15:3683
24. Wang X et al (2024) Organocatalytic enantioselective 1,12-addition of alkynyl biphenyl quinone methides formed in situ. Angew Chem Int Ed 63:e202400143
25. Wang S et al (2024) One-step construction of atropisomers bearing 1,5-central and axial chirality via catalytic diastereo- and atroposelective remote desymmetrizing alkynylation. ACS Catal 14:18872–18883

26. Tan X et al (2023) Enantioselective synthesis of tetraarylmethanes through *meta*-hydroxyl-directed benzylic substitution. Nat Synth 2:275–285
27. Wei W et al (2020) Diastereodivergent chiral aldehyde catalysis for asymmetric 1,6-conjugated addition and Mannich reactions. Nat Commun 11:5372
28. Qian D, Wu L, Lin Z, Sun J (2017) Organocatalytic synthesis of chiral tetrasubstituted allenes from racemic propargylic alcohols. Nat Commun 8:567
29. Chen M, Sun J (2017) Catalytic Asymmetric N-alkylation of indoles and carbazoles through 1,6-conjugate addition of *aza*-*para*-quinone methides. Angew Chem Int Ed 56:4583–4587
30. Chatupheeraphat A et al (2016) Asymmetric bronsted acid catalyzed substitution of diaryl methanols with thiols and alcohols for the synthesis of chiral thioethers and ethers. Angew Chem Int Ed 55:4803–4807
31. Wang Z, Wong YF, Sun J (2015) Catalytic asymmetric 1,6-conjugate addition of *para*-quinone methides: formation of all-carbon quaternary stereocenters. Angew Chem Int Ed 54:13711–13714
32. Xu D et al (2025) Catalytic asymmetric synthesis of inherently chiral eight-membered O-heterocycles through cross-[4 + 4] cycloaddition of quinone methides. Angew Chem Int Ed 64:e202416873
33. Hu X et al (2024) Catalytic enantioselective [4 + 2] cycloadditions of salicylaldehyde acetals with enol ethers. Angew Chem Int Ed 63:e202315759
34. Wu X, Sparr C (2022) Stereoselective synthesis of atropisomeric acridinium salts by the catalyst-controlled cyclization of *ortho*-quinone methide iminiums. Angew Chem Int Ed 61:e202201424
35. Gou B-B et al (2022) Modular construction of heterobiaryl atropisomers and axially chiral styrenes via all-carbon tetrasubstituted VQMs. Angew Chem Int Ed 61:e202208174
36. Suneja A, Loui HJ, Schneider C (2020) Cooperative catalysis for the highly diastereo- and enantioselective [4 + 3]-cycloannulation of *ortho*-quinone methides and carbonyl ylides. Angew Chem Int Ed 59:5536–5540
37. Trost BM, Zuo Z (2020) Highly regio-, diastereo- and enantioselective synthesis of tetrahydroazepines and benzo[*b*]oxepines through palladium-catalyzed [4 + 3] cycloaddition reactions. Angew Chem Int Ed 59:1243–1247
38. Sun M et al (2019) Catalytic asymmetric (4 + 3) cyclizations of in situ generated *ortho*-quinone methides with 2-indolylmethanols. Angew Chem Int Ed 58:8703–8708
39. Lee A et al (2019) Carbene-catalyzed enantioselective decarboxylative annulations to access dihydrobenzoxazinones and quinolones. Angew Chem Int Ed 58:5941–5945
40. Pandit RP, Kim ST, Ryu DH (2019) Asymmetric synthesis of enantioenriched 2-aryl-2,3-dihydrobenzofurans by a Lewis acid catalyzed cyclopropanation/intramolecular rearrangement sequence. Angew Chem Int Ed 58:13427–13432
41. Jiang F, Yuan F-R, Jin L-W, Mei G-J, Shi F (2018) Metal-catalyzed (4 + 3) cyclization of vinyl aziridines with *para*-quinone methide derivatives. ACS Catal 8:10234–10240

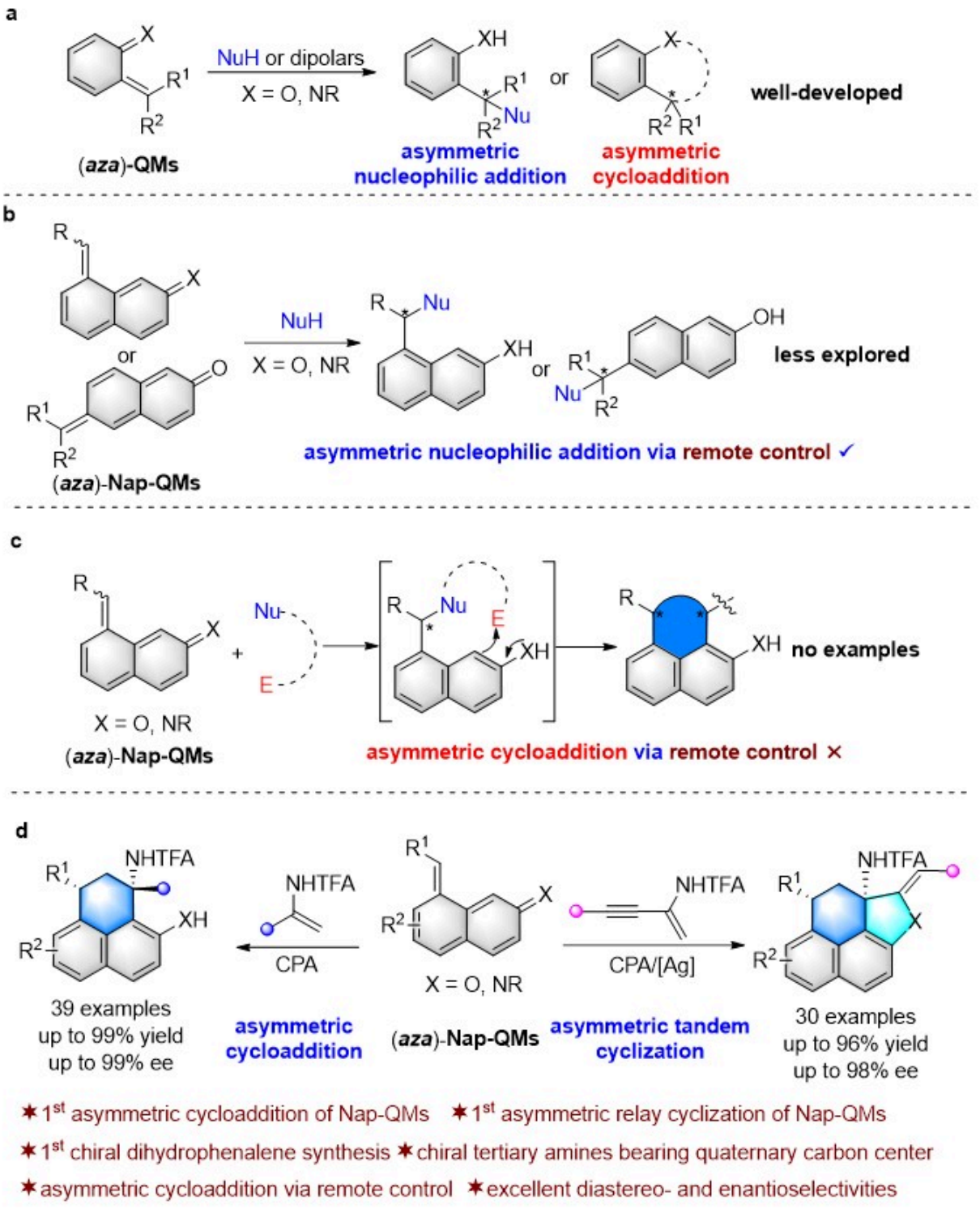
42. Lam H, Qureshi Z, Wegmann M, Lautens M (2018) Transition-metal-free [4 + 3]-cycloaddition of ortho-quinone methides and isomuenchnones: catalytic and diastereoselective assembly of oxa-bridged oxazocine scaffolds. Angew Chem Int Ed 57:16185–16189
43. Liu S, Chan KL, Lin Z, Sun J (2023) Asymmetric synthesis of remotely chiral naphthols and naphthylamines via naphthoquinone methides. J Am Chem Soc 145:12802–12811
44. Liu M, Shen B, Liu C, Yu P, Li P (2023) Organocatalytic enantioselective 1,8-addition for the synthesis of chiral tetraarylmethanes from 2–naphthol/naphthalen-2-amine based tertiary alcohols. J Am Chem Soc 145:14562–14569
45. Xu H-L et al (2025) Organocatalytic asymmetric synthesis of *o*–carboranyl amines. J Am Chem Soc 147:3692–3701
46. Liu M, Zhang Y, Ke X-Y, Ni S-F, Li P (2025) Asymmetric organocatalytic 1,6-conjugate addition of alkynyl 8–methylenenaphthalen-2(8*H*)–one formed in situ: synergistic construction of axial and central chirality. Org Lett 27:1271–1275
47. Shen K et al (2026) Organocatalytic enantioselective synthesis of axially chiral tetrasubstituted allenes via direct 1,8-addition to in situ formed alkynyl 8-methylenenaphthalen-2(8*H*)-ones. Org Lett 28:1374–1379
48. Yin Y-X et al (2025) Scandium triflate catalyzed cycloadditions of vinyl diazo compounds and in situ formed naphthoquinone methides. J Org Chem 90:6025–6030
49. Bouchet D, Varlet T, Masson G (2022) Strategies toward the difunctionalizations of enamide derivatives for synthesizing α, β substituted amines. Acc Chem Res 55:3265–3283
50. Varlet T, Masson G (2021) Enamides and dienamides in phosphoric acid-catalysed enantioselective cycloadditions for the synthesis of chiral amines. Chem Commun 57:4089–4105
51. Wang M-X (2015) Exploring tertiary enamides as versatile synthons in organic synthesis. Chem Commun 51:6039–6049
52. Gopalaiah K, Kagan HB (2011) Use of nonfunctionalized enamides and enecarbamates in asymmetric synthesis. Chem Rev 111:4599–4657
53. Matsubara R, Kobayashi S (2008) Enamides and enecarbamates as nucleophiles in stereoselective C–C and C–N bond-forming reactions. Acc Chem Res 41:292–301
54. Saha S, Schneider C (2015) Brønsted acid-catalyzed, highly enantioselective addition of enamides to in situ-generated *ortho*-quinone methides: a domino approach to complex acetamidotetrahydroxanthenes. Chem Eur J 21:2348–2352
55. Kretzschmar M, Hodík T, Schneider C (2016) Brønsted acid catalyzed addition of enamides to *ortho*-quinone methide imines—an efficient and highly enantioselective synthesis of chiral tetrahydroacridines. Angew Chem Int Ed 55:9788–9792
56. Wang T, Huang B, Wang Y-Q (2022) Enantioselective synthesis of spiro chroman-isoindolinones via formal (4 + 2) cycloaddition of in situ-generated ortho-quinone methides with 3-methylene isoindolinones. Adv Synth Catal 364:2596–2605

57. Distrutti E et al (2009) A nitro-arginine derivative of trimebutine ($NO_2$-Arg-Trim) attenuates pain induced by colorectal distension in conscious rats. Pharmacol Res 59:319–329
58. Maurice T et al (2019) Neuroprotection in non-transgenic and transgenic mouse models of Alzheimer's disease by positive modulation of σ1 receptors. Pharmacol Res 144:315–330
59. Zhang J-L, He W-B, Hu X-Q, Xu P-F (2024) New strategies for asymmetric photocatalysis: asymmetric organocatalytic/photoredox relay catalysis for efficient synthesis of polycyclic compounds containing vicinal amino alcohols. *Sci. China Chem*. 67, 945 – 952
60. Bao M, Zhou S, Hu W, Xu X (2022) Recent advances in gold-complex and chiral organocatalyst cooperative catalysis for asymmetric alkyne functionalization. Chin Chem Lett 33:4969–4979
61. Du Z, Shao Z (2013) Combining transition metal catalysis and organocatalysis – an update. Chem Soc Rev 42:1337–1378
62. Hölscher D (2006) Monolaterol, the First Configurationally Assigned Phenylphenalenone Derivative with a Stereogenic Center at C-9, from Monochoria elata. J Nat Prod 69:1614–1617
63. Wang M-Z et al (2018) Concise Synthesis of natural phenylphenalenone phytoalexins and a regioisomer. J Nat Prod 81:98–105
64. Kimura T et al (2019) New tetrahydroquinoline and indoline compounds containing a hydroxy cyclopentenone, virantmycin B and C, produced by streptomyces sp. AM-2504. *J. Antibiot.* 72, 169 – 173
65. Matsunaga N et al (2004) C17,20-lyase inhibitors. Part 2: Design, synthesis and structure–activity relationships of (2-naphthylmethyl)-1*H*-imidazoles as novel C17,20-lyase inhibitors. Bioorg Med Chem 12:4313–4336
66. Adams JL et al (1996) Bicyclic N-hydroxyurea inhibitors of 5-lipoxygenase: pharmacodynamic, pharmacokinetic, and in vitro metabolic studies characterizing *N*-Hydroxy-*N*-(2,3-dihydro-6-(phenylmethoxy)-3-benzofuranyl)urea. J Med Chem 39:5035–5046
67. Tercel M et al (2003) Unsymmetrical DNA cross-linking agents: combination of the CBI and PBD pharmacophores. J Med Chem 46:2132–2151
68. Zhu X-Q, Wang Q, Zhu J (2023) Organocatalytic enantioselective Diels-Alder reaction of 2-trifluoroacetamido-1,3-dienes with α,β-unsaturated ketones. Angew Chem Int Ed 62:e202214925
69. Zhu X-Q, Wang Q, Wodrich MD, Zhu J (2025) Chiral phosphoric acid-catalyzed enantioselective higher-order cycloadditions: temperature-dependent periselectivity. J Am Chem Soc 147:26165–26176
70. Man N et al (2021) Synthesis of chiral propargylamines, chiral 1,2-dihydronaphtho[2,1-*b*]furans and naphtho[2,1-*b*]furans with C-alkynyl *N,N'*-di-(tert-butoxycarbonyl)-aminals and β-naphthols. Chem Eur J 27:12884–12889

# Tables

Tables 1 and 2 are available in the Supplementary Files section.

# Figures




## Figure 1

**Asymmetric Reaction of Quinone Methides (QMs) and Naphthoquinone Methides (Nap-QMs). a**. Asymmetric nucleophilic addition and cycloaddition of (*aza*)-QMs. **b**. Asymmetric nucleophilic addition

of (*aza*)-Nap-QMs. **c**. Our hypothesis: asymmetric cycloaddition of (*aza*)-Nap-QMs. **d.** This work: CPA-catalyzed asymmetric cycloaddition and tandem cyclization reaction of (*aza*)-Nap-QMs.

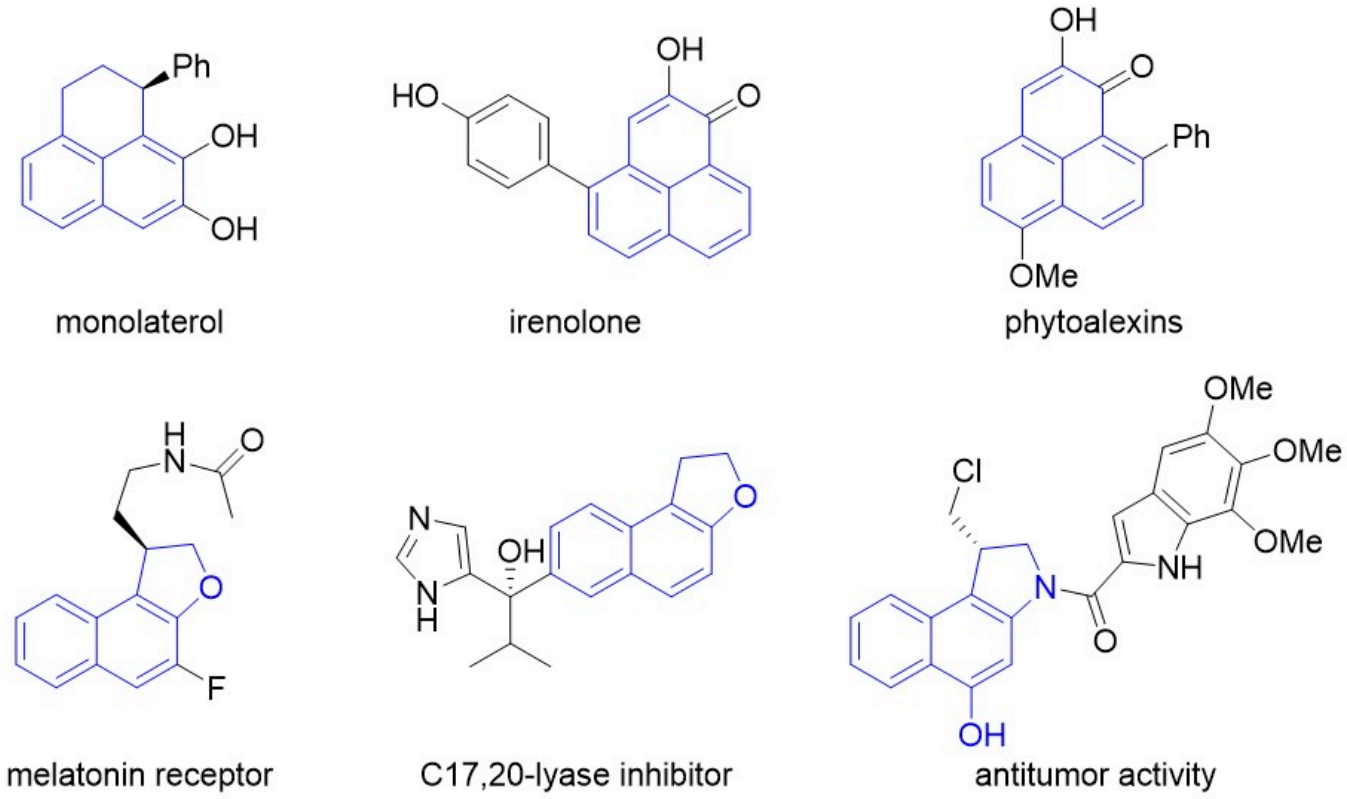
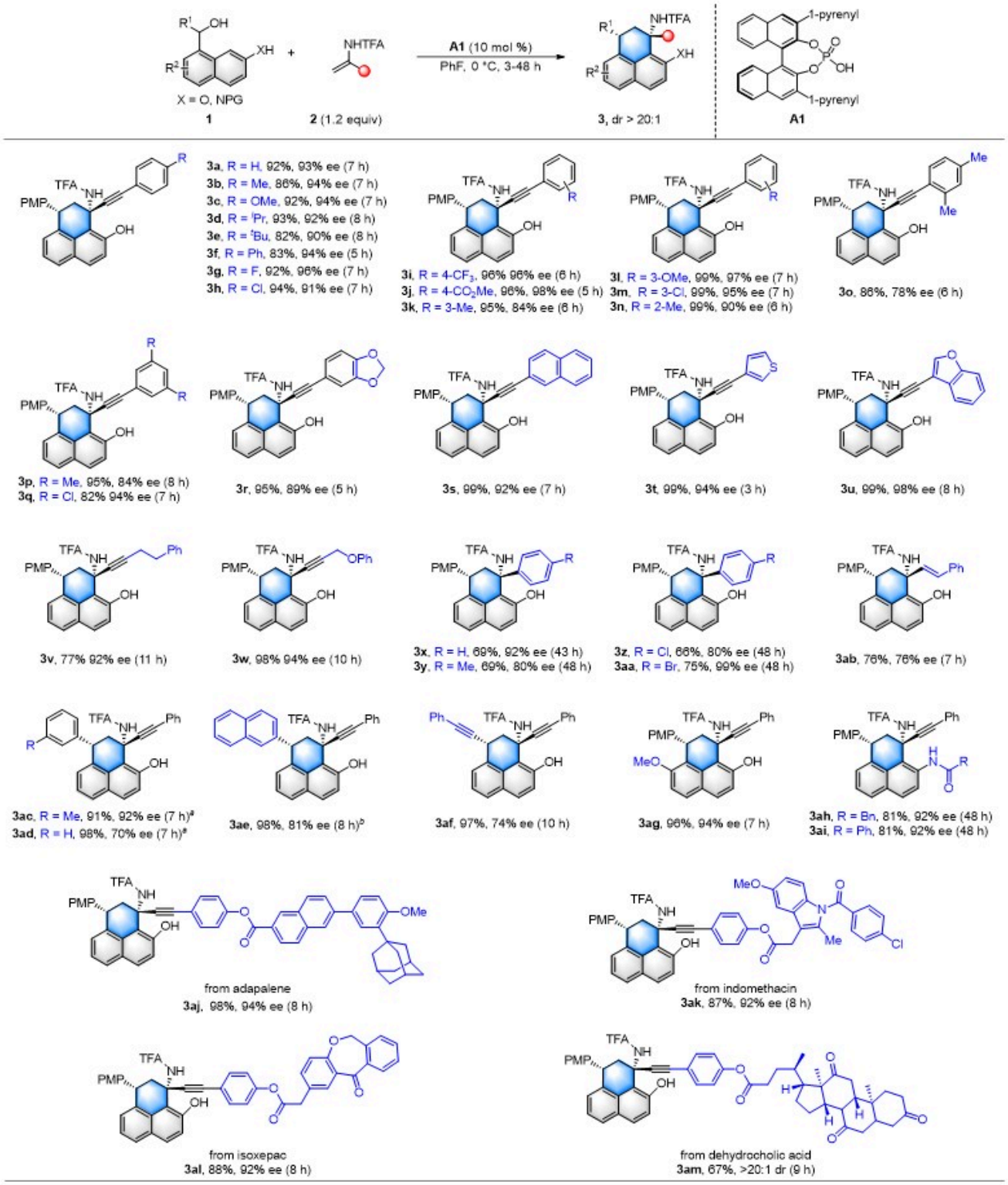


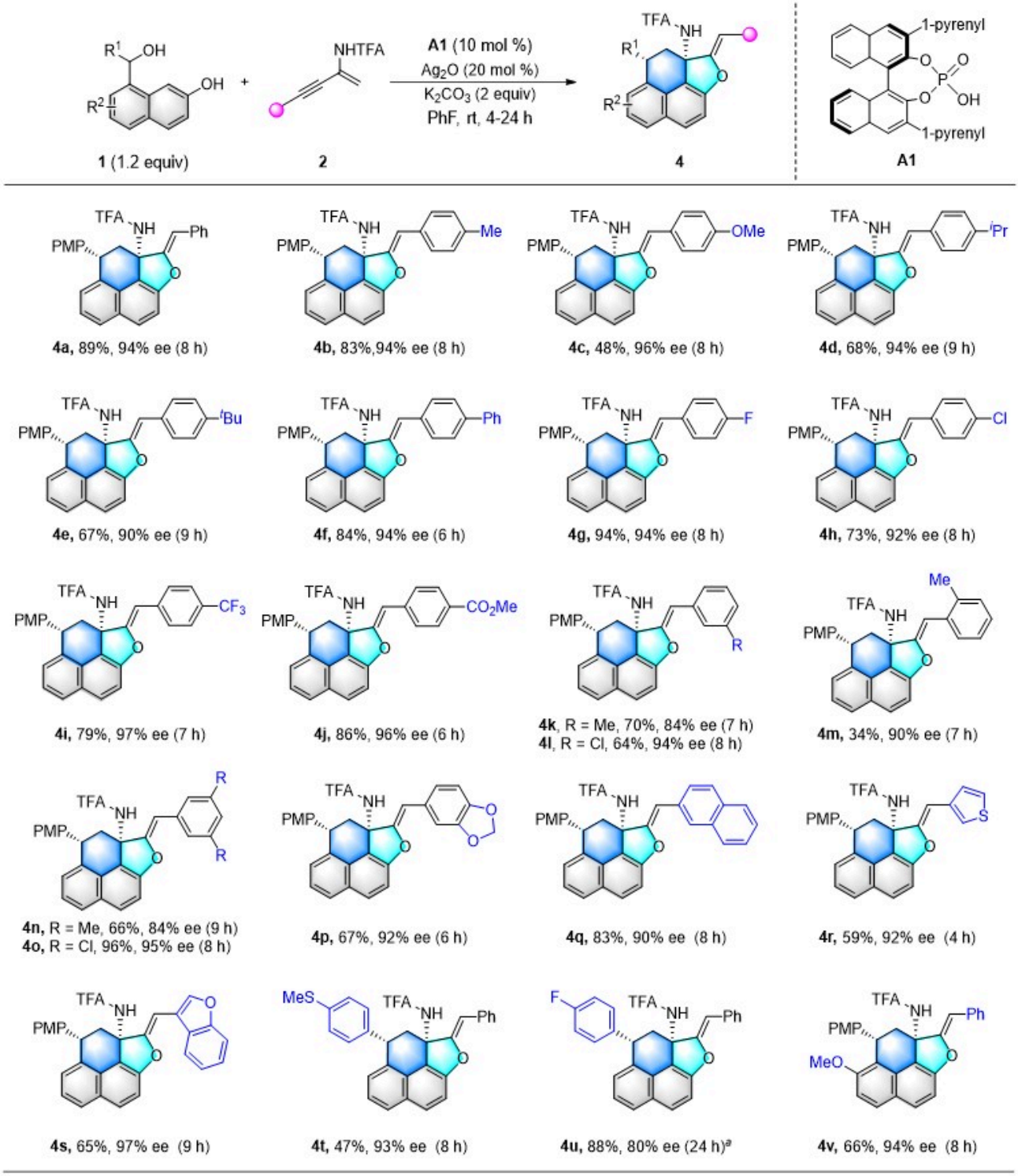

**Figure 2**

**Selected natural products and bioactive moleculescontaining phenalene, dihydronaphtho[2,1-*b*]furan and 1,2-dihydrobenzo[*e*]indole motif.** Some of representative molecules are listed.



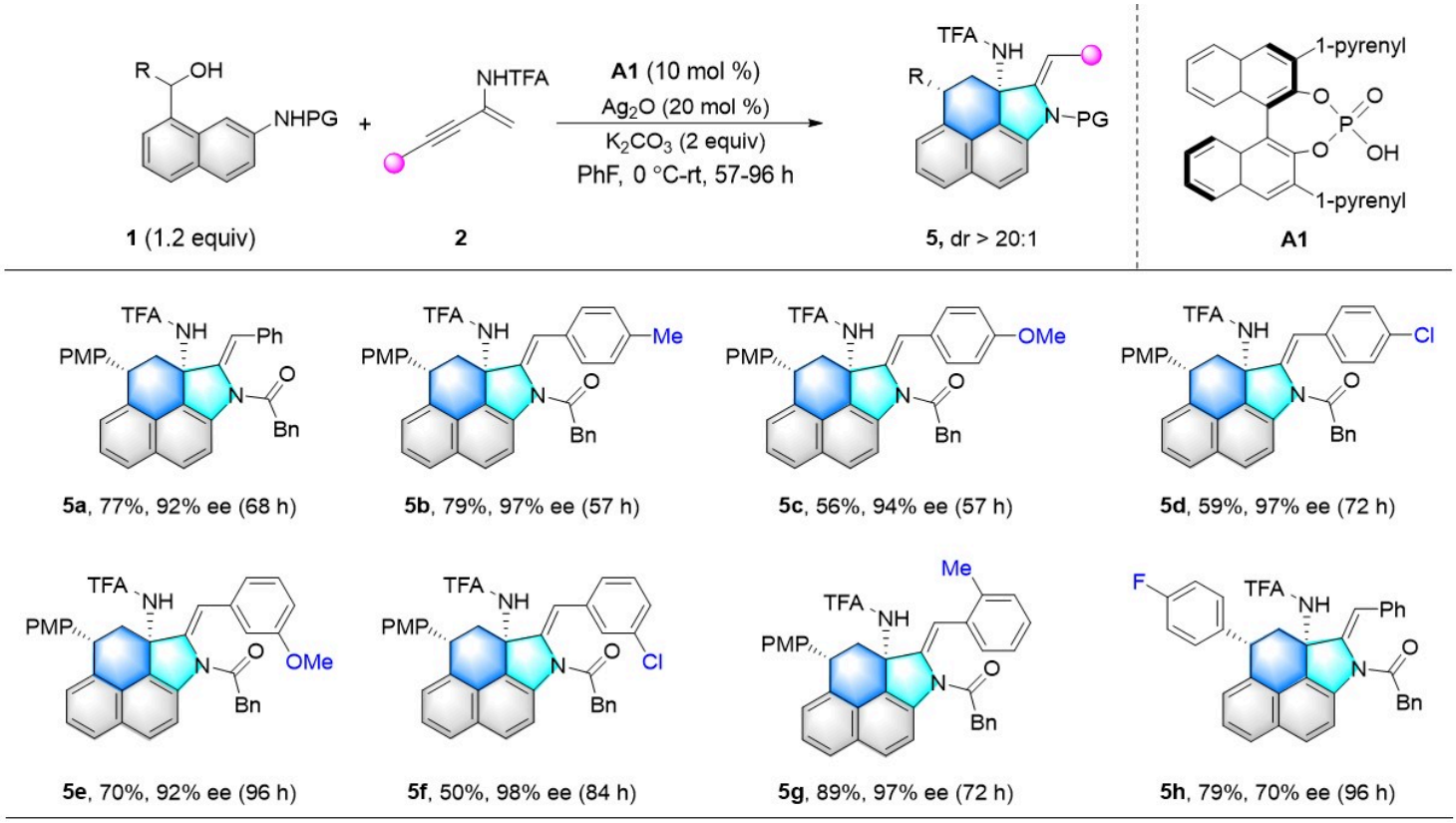

## Figure 3

**Scope of asymmetric cycloaddition of Nap-QMs with enamides.** Reaction conditions: **1** (0.2 mmol), **2** (0.24 mmol), CPA **A1** (10 mol %) in PhF (2 mL) at 0 °C, 3-48 h. [a]**A10** (10 mol %) was used as catalyst, 0 °C. [b]**A10** (10 mol %) was used as catalyst, -35 °C.



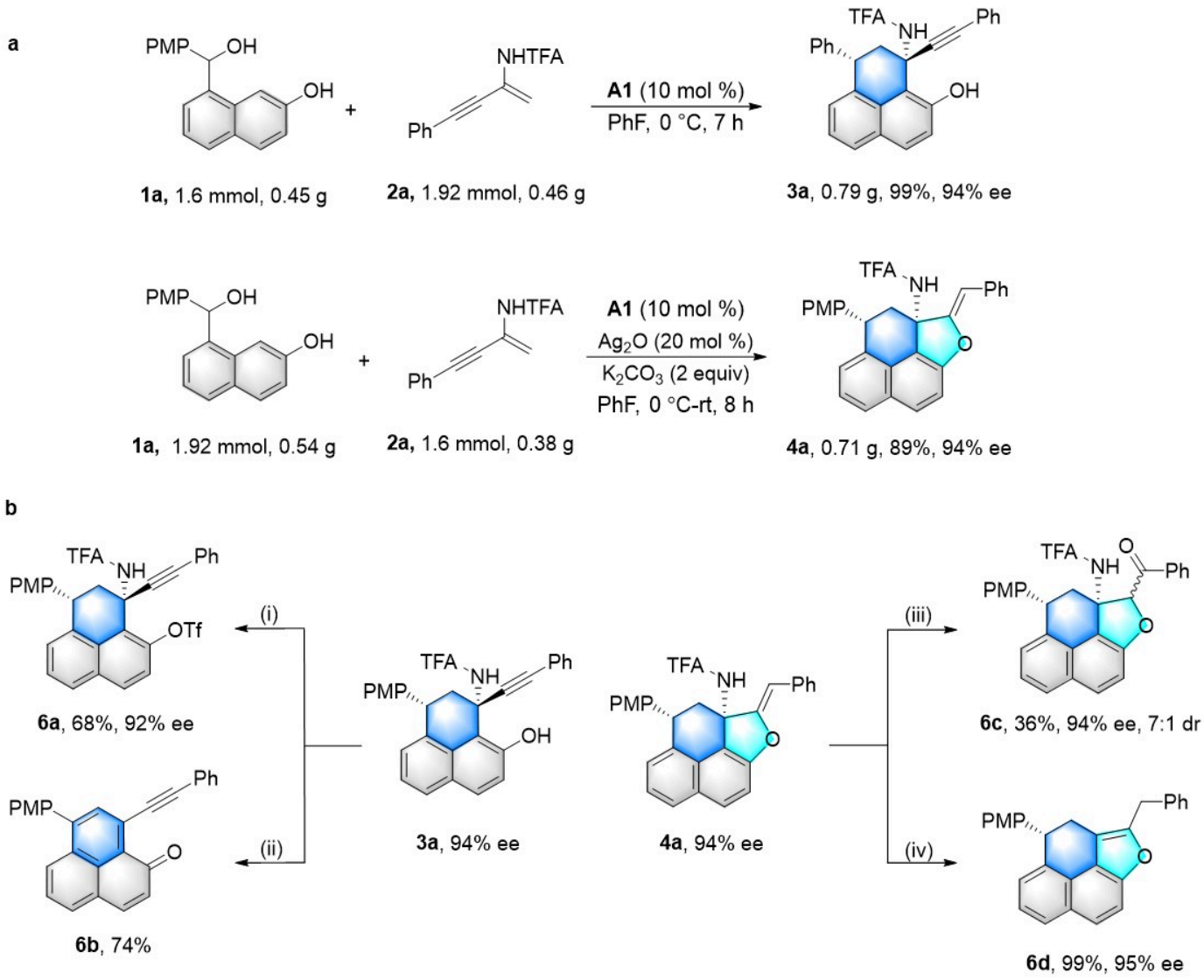

## Figure 4

**Scope of asymmetric relay of Nap-QMs 1.** Reaction conditions: **1** (0.24 mmol), **2** (0.2 mmol), CPA **A1** (10 mol %) in PhF (4 mL) at 0 °C; then adding $Ag_2O$ (0.04 mmol) at rt. [a]**A10** (10 mol %) was used as catalyst, -35 °C.



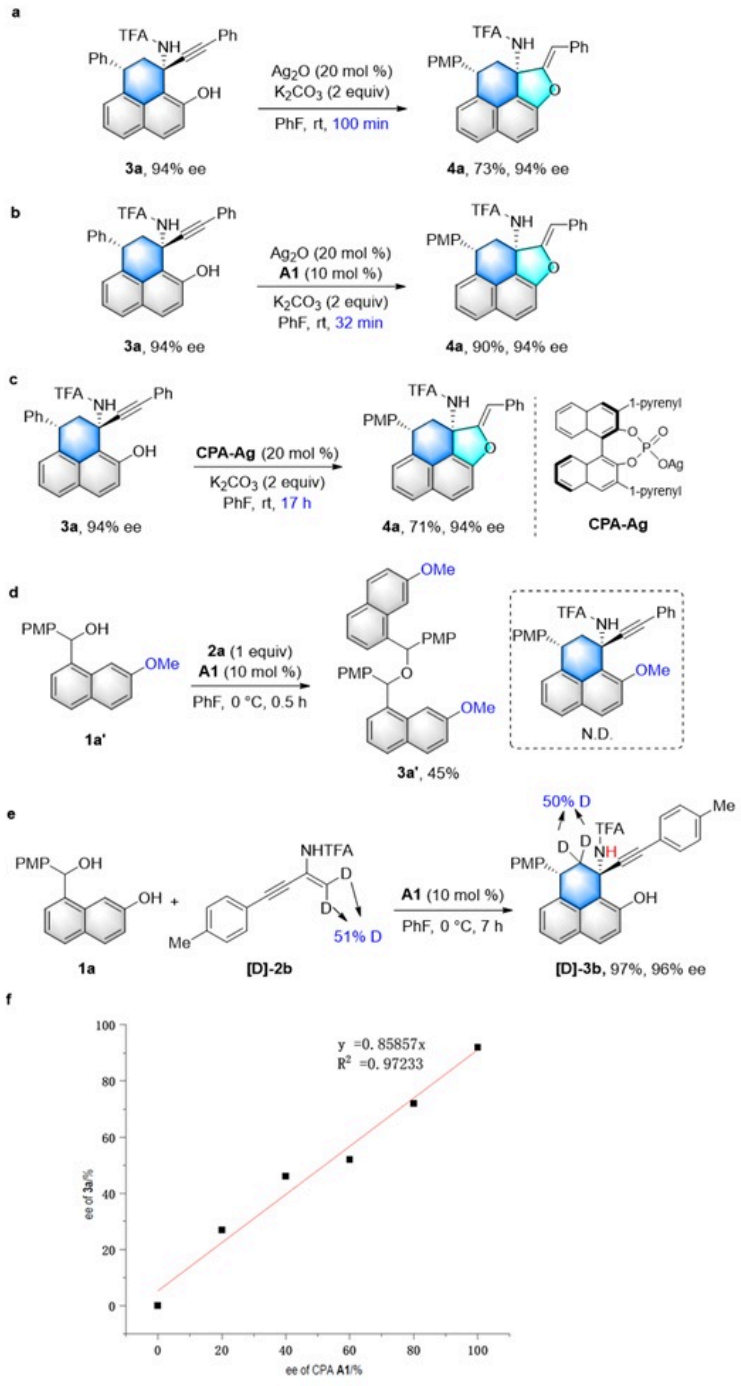

## Figure 5

**Scope of asymmetric relay of *aza*-Nap-QMs 1.** Reaction conditions: **1** (0.24 mmol), **2** (0.2 mmol), CPA **A1** (10 mol %) in PhF (4 mL) at 0 °C; then adding $Ag_2O$ (0.04 mmol) at rt.




## Figure 6

**Scale-up reaction and product elaborations. a**. Preparative-scale reaction of **1a**. **b**. Synthetic applications of **3a** and **4a**. Reagents and conditions: (i) $Tf_2O$ (1 equiv), $Et_3N$ (1 equiv), DCM, rt, 50 min. (ii) $Cs_2CO_3$ (1.5 equiv), PhF, rt, 70 min. (iii) $NaIO_4$ (4 equiv), $RuCl_3$ (7 mol %), THF:MeCN:$H_2O$ (2:1:1), rt, 15 min. (iv) $Et_3SiH$ (2 equiv), $BF_3$•$Et_2O$ (4 equiv), DCM, rt, 30 min.




## Figure 7

**Control experiment. a**. Ag-catalyzed cyclization of **3a**. **b**. Ag/CPA-cocatalyzed cyclization of **3a**. **c**. CPA-Ag-catalyzed cyclization of **3a d**. CPA-catalyzed reaction of methyl protected naphthol **1a'** with enamide **2a**. **e**. CPA-catalyzed cyclization of naphthol **1a** with enamide [D]-**2b**. **f**. Non-linear effect of CPA catalyst.

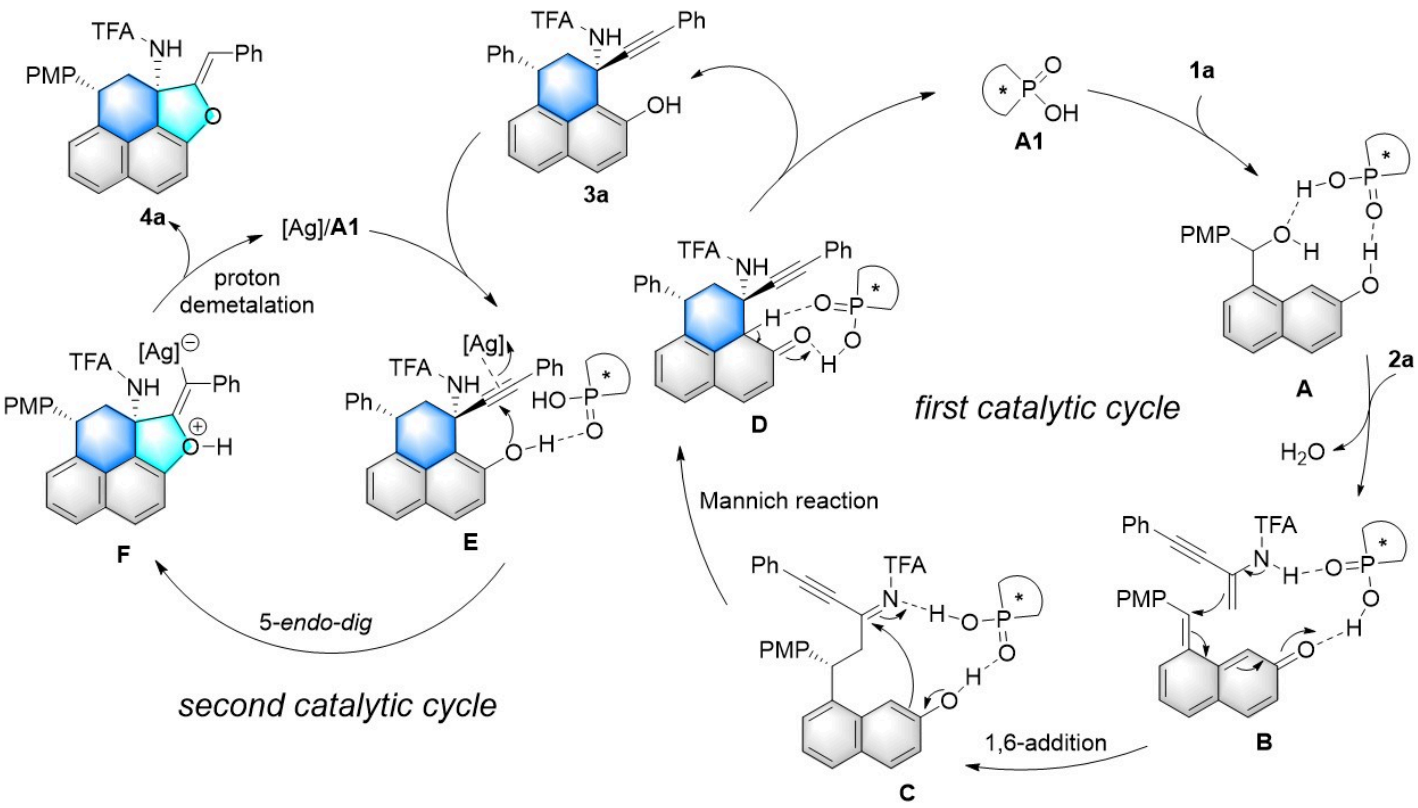



**Figure 8**

**Proposed reaction mechanism.** Mechanism for the CPA-catalyzed asymmetric [4+2] cycloaddition of Nap-QMs.

# Supplementary Files

This is a list of supplementary files associated with this preprint. Click to download.

- 4v.cif
- SIall.pdf
- graphicalabstract.jpg
- tables.docx